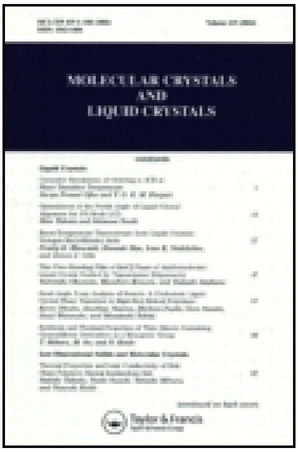

Molecular Crystals and Liquid Crystals
Publication details, including instructions for authors and subscription information:
http://www.tandfonline.com/loi/gmcl20

Effect of Thickness Variation and LiF Interlayer of the Conjugated Polymer/Fullerene Photoactive Layers on the Optical and Electrical Performance of Solar Cell Devices

Sang Ouk Ryu [a]

[a] Department of electronics engineering, Dankook University, San #29, Anseo-dong, Cheonan-si, Chungcheongnam-do, 330-714, South Korea

Version of record first published: 18 Oct 2011

To cite this article: Sang Ouk Ryu (2011): Effect of Thickness Variation and LiF Interlayer of the Conjugated Polymer/Fullerene Photoactive Layers on the Optical and Electrical Performance of Solar Cell Devices, Molecular Crystals and Liquid Crystals, 551:1, 154-162

To link to this article: http://dx.doi.org/10.1080/15421406.2011.600638

Mol. Cryst. Liq. Cryst., Vol. 551: pp. 154–162, 2011

ISSN: 1542-1406 print/1563-5287 online
DOI: 10.1080/15421406.2011.600638

Effect of Thickness Variation and LiF Interlayer of the Conjugated Polymer/Fullerene Photoactive Layers on the Optical and Electrical Performance of Solar Cell Devices

SANG OUK RYU*

Department of electronics engineering, Dankook University, San #29,
Anseo-dong, Cheonan-si, Chungcheongnam-do, 330-714, South Korea

We fabricated organic solar cell (OSC) devices using blended solution of MDMO-PPV:PCBM-C_{61}. The electrical properties of the devices were investigated as a function of the photoactive layer thicknesses and by addition of LiF interlayer. The devices having photoactive layer under 200nm has shown the best efficiency. The electrical characteristics were degraded by decreasing photoactive layer thicknesses. The devices with 200nm of photoactive layer without LiF interlayer have shown the best electrical characteristics, which were 0.49% of PCE, 41.5% of fill factor and 1.4mA/cm^2 of J_{SC}. Similar trends were observed by adding LiF interlayer between active layer and Al cathode. As a result, the efficiency of the OSC devices was more enhanced by adding LiF interlayer. The power conversion efficiency was improved up to 32% (PCE = 0.65%) when compared with the devices without LiF interlayer (PCE-0.49%).

Keywords: OSC; blended solution; a function of the photoactive layer thicknesses; LiF interlayer

Introduction

Photovoltaic (PV) cells have become more and more attractive as a truly clean, renewable energy source. The biggest obstacle of the crystalline silicon-based solar cell is the high semiconductor manufacturing cost. Polymer-based solar cell devices have shown promising potential as an alternative energy source [1]. Some of the important advantages of these polymer-based organic solar cells (OSCs) include low cost of fabrication, apply to the large area, ease of processing, mechanical flexibility and versatility of chemical structure from advances in organic chemistry [2]. However, low efficiency of these OSCs comparing to silicon based solar cells, limits their feasibility for commercial use [3]. The efficiencies of OSC devices are mainly limited by several factors. For example, the high energy band gap of the materials used also limits the capability to harvest the photo generated charges with lower energy from the sunlight. More importantly, the charge carrier mobility of organic materials is very low. The poor conductivity of organic thin films cuts down the output power conversion efficiency significantly [4, 5]. The efficiencies of polymer solar cells got a major increase with the introduction of the bulk-heterojunction (BHJ) concept consisting of an interpenetrating network of electron donor and acceptor materials [6, 7]. This concept

---

*Corresponding author. E-mail: ryuso@dankook.ac.kr has also been demonstrated in small-molecular OSCs [8]. For the poly(3-hexylthiophene) based polymer OSCs using this structure highest efficiencies reaching up to 5% have been reported [9]. The BHJ structure provides not only high surface contacts for charge separation, but also an interpenetrating network for efficient charge transport [10].

The essential parameters of PV cells which determine power conversion efficiency (PCE) are open circuit voltage (V_{OC}, (m)V), short circuit current density (J_{SC}, mA/cm^2), and fill factor (FF,%). Recently, many of groups have studied much effort to enhance these parameters. For example, transparent and tandem or stacking structures to enhance the efficiency, narrow band gap polymer materials, and using triplet compounds as active materials [11–13].

The basic mechanisms of photovoltaics are light absorbing and photo carrier generating. More light absorption tends to generate more photon carriers which contribute to increasing J_{SC} and PCE. Also the light absorption intensity depends on the thickness of photoactive layer. But, generally, PCE seems to be degraded when the photoactive layer thickness increase to some degree so that, the modeling of photoactive layer thicknesses is very important to improve PCE of photovoltaics [14]. Recent progress on OSCs utilizing compound of MDMO-PPV:PCBM was reported that the PCE of 2.5% under air mass (AM) 1.5 illumination included a strategy of incorporating a small amount of LiF at the interface between the photoactive layer and the metal cathode [3]. This technique has previously been used to enhance the performance of organic light emitting diodes (OLEDs) for devices fabricated either by thermal deposition of low molecular weight compounds or by solution casting of polymers [15, 16]. This LiF interlayer has well known to the dipole interaction, lower of the Al work function, and protect organic layer from hot Al atoms. These effects can attribute to enhancement of electrical performances.

In this study, we have characterized the electrical performances of OSCs based on BHJ structure including LiF interlayer. We analyzed the electrical characteristics by varying the photoactive thicknesses and adding LiF interlayer. The [6,6]-phenyl C61-butyric acid methyl ester (PCBM-C_{61}, 99%) was used as an electron acceptor which has 284–341nm of absorption wavelength. And poly[2-methoxy-5(3,7-dimethyloctyloxy-1,4-phenylenevinylene)] (MDMO-PPV) was used as an electron donor which has maximum 509nm of absorption wavelength. These materials were obtained from American dye source (ADS). Also PEDOT:PSS was used as an hole injection layer (HIL) which was obtained from Baytron P. (AI 4083).

Experimental

The fabricated OSCs used in this study consist of a photoactive layer of MDMO-PPV:PCBM-C_{61} based on BHJ structure. The photoactive material, MDMO-PPV and PCBM- C_{61} were prepared by dissolving in toluene(0.5 wt-%) and stirred for 10 hours to ensure complete dissolution. The MDMO-PPV and PCBM solutions were mixed at a ratio of 1:4 by weight. The ratio of 1:4 was obtained from previous studies about the efficiency variation as a function of the material concentration. The ITO coated soda lime glass was patterned with acid and cleaned using acetone, methanol and de-ionized water in an ultrasonic bath to remove contaminants on the substrates. And then iso-propyl alcohol (IPA) cleaning was used to remove the water pollutants. The cleaned ITO substrates were treated by plasma surface treatment with $O_2/Ar = 2/1$ mixture for 1minute. The power of 150W RF condition was used to improve the interface conditions between organic material and ITO, and to remove the native-oxide film on ITO substrate. The polyethylenedioxythiopene:

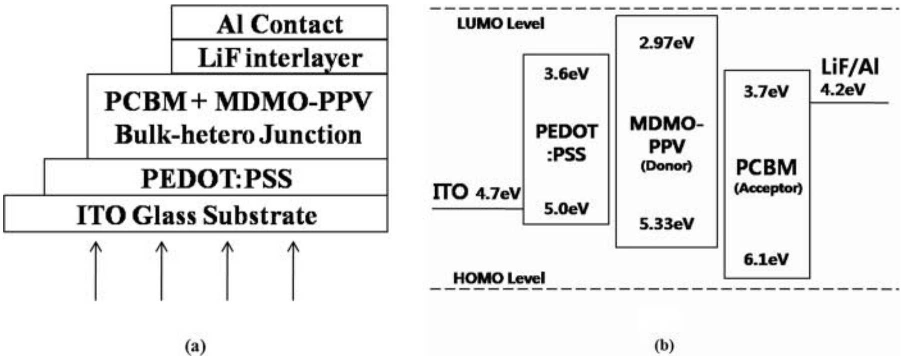

Figure 1. (a) A cross sectional view of the fabricated devices (b) energy band gap diagram of OSC device fabricated in this study.

poly-styrenesulfonate (PEDOT:PSS) as a hole injection layer (HIL) was deposited using spin coating method on the ITO substrate and baked at 90°C for 1hour. And the photoactive layer was spin coated with different spin speed (500, 1000, 2000rpm) to have different thicknesses for each samples. The coated samples were then baked at 90°C for 30min to evaporate the solvents. At coating process 500rpm was the lowest spin speed we could manipulate to obtain the high quality thin films. Therefore we set the spin speed range from 500rpm to 2000 rpm. After photoactive layer was coated, small amount of LiF (0.5nm) / Al (120nm) and pristine Al (120nm) metal electrode were evaporated subsequently under high vacuum conditions of 5×10^{-8} torr by SUNICELL PLUS 200. All the fabricated devices were post-annealed in vacuum oven at 110°C for 20min. The solution stirring and spin coating were conducted in the ambient conditions.

The fabricated devices were classified as photoactive layer thicknesses and existence of LiF interlayer. The light absorption layers had the same dimension of 2×2 mm^2. The fabricated solar cell structures and energy band diagrams are shown in Figure 1. The optical absorption spectrum was investigated by means of UV-vis spectroscopy (UV 1601PC UV-visible Photometer). The power conversion efficiencies (PCE) were calculated from the current density-voltage (J-V) characteristics and fill factor (FF) under a solar simulated light irradiation of 100mW/cm^2 in the ambient condition (ORIEL solar simulator with 150W Xe lamp and KEITHLY SMU 2400). Before the devices were measured, the light source has been calibrated by reference cell (ORIEL Solar reference cell). The external quantum efficiency (EQE) was measured by ORIEL IQE 200 for each fabricated devices.

Results and Discussion

The chemical structures of the materials which have been used in this study are shown in Figure 2. These materials are well known to have good absorption characteristics at a range of visible ray (MDMO-PPV: maximum 509nm, PCBM-C_{61}: 284–341nm). By utilizing those active layers, BHJ device structure has been studied. The structure of devices and the energy band diagram of each layer are depicted in Figure 1. To overcome one of the main limitation factors, i.e., charge separation problem in the organic photovoltaic devices the BHJ structure was used. After evaporating LiF/Al or Al contact layer, the fabricated devices were annealed at 110°C for 20min. The effect of post-annealing process has been reported by H. Hoppe et al. and Chirvase et al. [17, 18]. According to the report, the performance

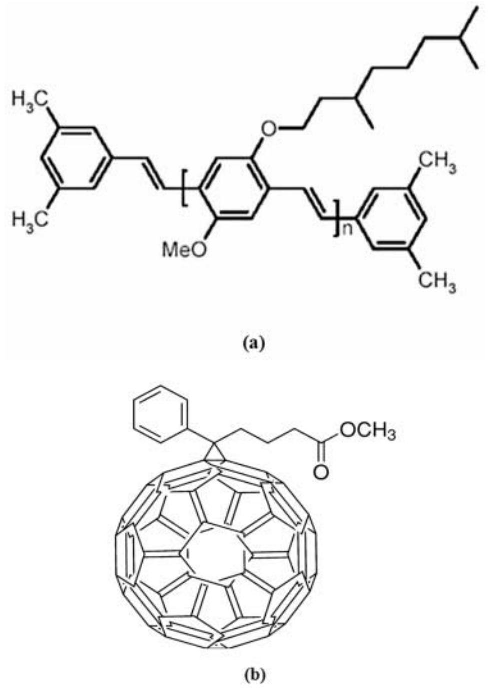

Figure 2. Chemical structures of (a) MDMO-PPV, (b) PCBM-$C_{61.}$

of the photoactive layer could be degraded at high temperatures caused by large PCBM aggregating. We have already optimized the annealing temperature and duration (110°C and 20min.) at the previous study to enhance the electrical performances and adhesion improvement between organic layer and metal cathode.

Figure 3 shows the J-V characteristics of the fabricated devices having Al-only electrode as a function of photoactive thicknesses. The thickness of active layer was measured by ellipsometer and the thickest layer was around 200nm. We observed that the thicker active layer (200nm) tends to show better efficiency characteristics. The highest performances were as follows; $J_{SC} = 1.4\text{mA/cm}^2$, $V_{OC} = 0.87\text{V}$, FF = 41.5%, PCE = 0.49%. Comparing to the thinner thickness device (90nm), the performances (V_{OC} and J_{SC}) were much improved. As a result, the calculated PCE was increased from 0.41% to 0.49%. Figure 4 shows the UV absorption intensities as a function of the photoactive layer thicknesses. According to the Lambert-Beer law;

$$A = kt, \tag{1}$$

where, A is the absorption intensity for a given wavelength, k is the absorption coefficient and t is the thickness of absorbent substance. The absorption coefficient, k is characteristic of the materials. In this study, we varied the thicknesses (t factors) of the photoactive layers. We observed that the absorption intensities were increased as thickening of the active layers. The intensity at 200nm photoactive layer thickness device has the highest absorption property comparing to other thickness devices (the PCBM peak = around 320nm, the MDMO-PPV peak = around 480nm). Generally, more light absorption can make more photo generated

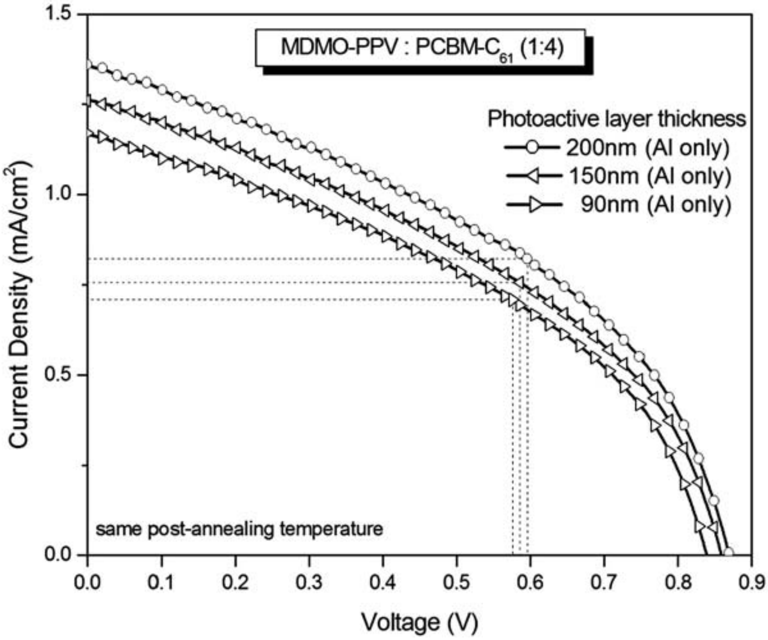

Figure 3. Current density-Voltage (J-V) characteristics of the fabricated devices with Al-only cathode as a function of photoactive layer thicknesses.

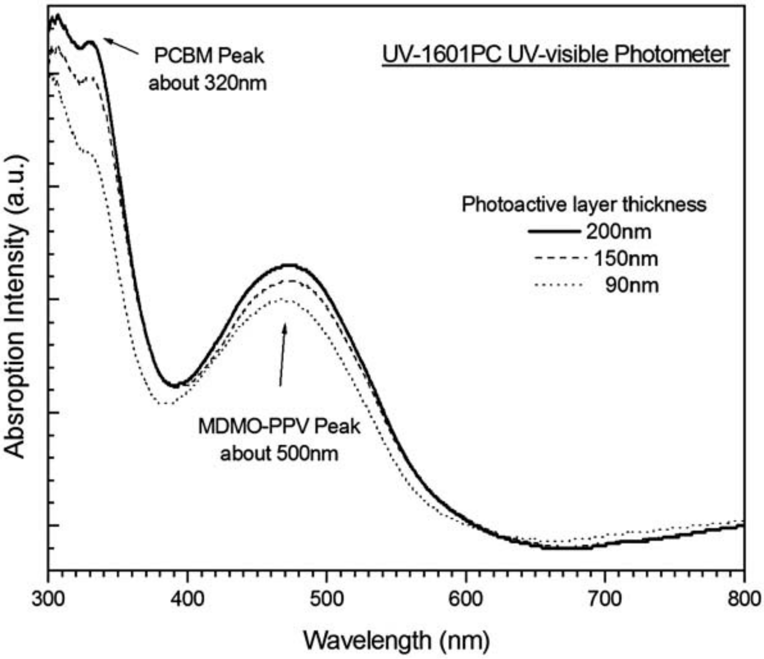

Figure 4. UV absorption intensity curves as a function of photoactive layer thicknesses.

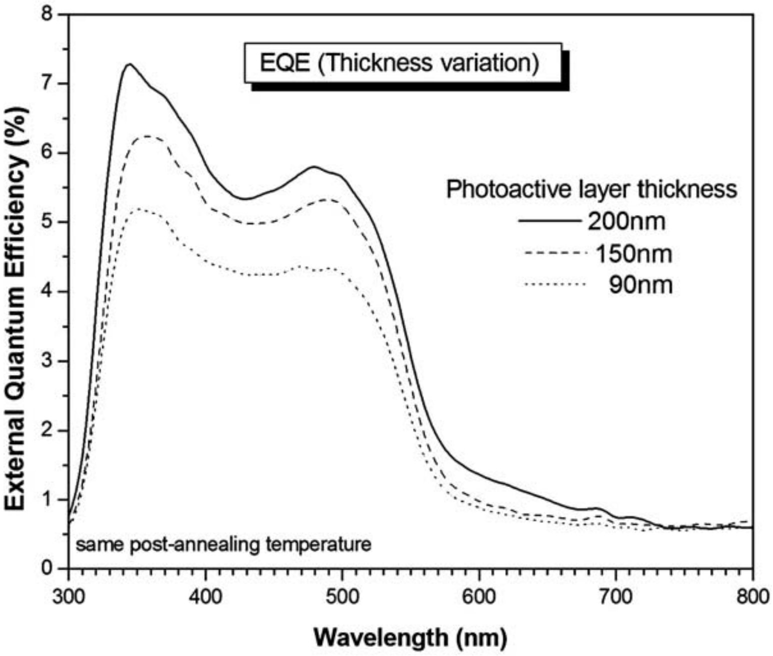

Figure 5. External quantum efficiency (EQE) curves as a function of photoactive layer thicknesses.

charges. Therefore the electrical characteristics could be improved at the thicker photoactive layer. In the previous study, M. Lenes *et al.* have reported that increasing the photoactive layer thickness does not necessarily result in a higher power conversion efficiency because the increase in short circuit current is canceled by a decrease in the fill factor. They also insisted that the decrease in the fill factor originates from the occurrence of a space-charge limited regime in the photocurrent and the recombination losses [14]. However, in this study, fabricated devices were much thinner than previous study and loss of fill factor was not detected. We think that the power conversion efficiency decrease by a reduction of the fill factor due to the increase of recombination losses may be compensated with higher light absorption characteristics, therefore higher density of generated free charge carriers.

Figure 5 shows the external quantum efficiency (EQE) of the fabricated devices. We could observe that the maximum QE occurred at the same peak around 320nm and 480nm of wavelength. The QEs also tend to show different results as a function of photo active layer thicknesses. In general, the QE follows this conventional equation,

$$\mathrm{QE} = hc\mathrm{SR}/q\lambda \tag{2}$$

where h: plank constant, c: light speed, SR: spectral response, q: quantity of electric charge, λ: the wavelength. From this equation, thickness of a photo-active layer is not a judging factor to the QE. However, the external quantum efficiency measurement is based on the collected electrons and holes through cathode and anode materials. If a normalization process against incoming light intensity or light absorption function of a cell was not conducted during calculation process the resulting quantum efficiency could be affected due to a physical function, for example, photon absorption intensity. Therefore, as shown

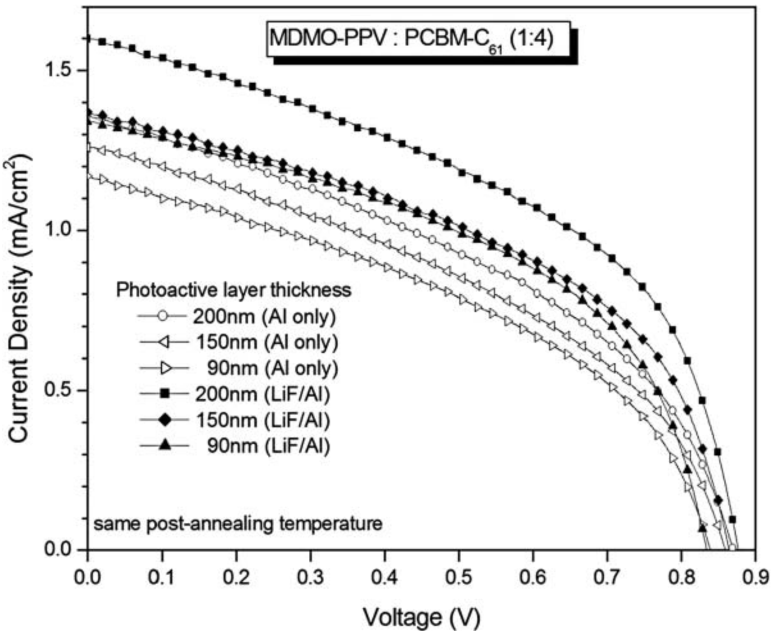

Figure 6. Current density-Voltage (J-V) characteristics of the fabricated devices including LiF interlayer (filled mark indicates cells with LiF interlayer).

in Fig. 4, the different thickness of active layer has different ability to absorb incoming photon, which may influence external quantum efficiency in Fig. 5.

Figure 6 shows the J-V characteristics of the devices including LiF interlayer and Al-only electrode. The electrical characteristics of the investigated devices are summarized in Table 1. We observed an improvement of essential parameters of power conversion efficiency for the LiF/Al electrode devices. Although the electrical characteristics of LiF/Al electrode devices were similar with the one having pristine Al only devices, the series resistance (R_{series}), especially, showed drastic decrease for the devices including LiF interlayer. Therefore, resulting fill factor and PCE of the device exhibited great improvement. The J_{SC}, FF, and PCE were 1.6mA/cm^2, 46.4%, and 0.65% for the device including LiF interlayer

Table 1. short circuit current density (J_{SC}), open circuit voltage (V_{OC}), fill factor (FF), and power conversion efficiency (PCE) of each devices processed at the different post-annealing temperatures

Thicknesses Contact	200nm Al	150nm Al	90nm Al	200nm LiF/Al	150nm LiF/Al	90nm LiF/Al
J_{SC} (mA/cm^2)	1.4	1.3	1.2	**1.6**	1.4	1.3
V_{OC} (V)	0.87	0.86	0.84	**0.88**	0.87	0.84
Fill Factor (%)	41.5	40.8	41.7	**46.4**	46	47.1
PCE (%)	0.49	0.44	0.41	**0.65**	0.55	0.53
R_{series}(kΩ)	3.24	3.12	3.37	**1.97**	2.19	2.1
R_{shunt}(kΩ)	37.5	39.54	41.57	**35.23**	44.70	43.03

and 1.4mA/cm^2, 41.5%, and 0.49% with pristine Al-only electrode, which improved about 32% in PCE.

Several mechanisms of LiF interlayer have been suggested, (i) lowering of the effective work function of the aluminum; (ii) dissociation of the LiF and subsequent chemical reaction (doping) of the organic layer; (iii) formation of a dipole layer leading to a vacuum level offset between the organic layer and the Al; and (iv) protection of the organic layer from the hot Al atoms during thermal deposition [19]. In this study, a little amount of increase was observed in the electrical properties (J_{SC}, V_{OC}) when compared between pristine Al cathode and LiF/Al cathode, but great increase in the fill factors for the devices including LiF interlayer. The LiF interlayer may affect to the interfacial property by which series resistances (R_{series}) were greatly decreased. The R_{series} was decreased from 3.24kΩ to 1.97kΩ when LiF interlayer is introduced. Because the fill factor is mainly affected by the series resistance the decrease of series resistance attribute to the overall efficiency increase of the photovoltaic cells.

Although overall efficiency performance of devices prepared in this report is not the best value ever reported the energy conversion performance could be increased after proper sample passivation throughout the whole process.

Conclusions

We have studied about the electrical characteristics of MDMO-PPV:PCBM-C_{61} OSCs based on BHJ structure as a function of photoactive layer thicknesses including LiF interlayer. The energy conversion efficiency was improved when thicker photoactive layer and LiF interlayer were introduced. The observed PCE for the 200nm photoactive layer having LiF interlayer was 0.65%, which was about 32% improvement. We think that the photoactive layer thickness can be mainly contributed to light absorption intensity and it also affects to generate the photon carriers. Furthermore, by inserting the LiF interlayer, the interface property was greatly improved between organic layer and Al cathode, in turn, series resistance was decreased. As a result, the electrical characteristics, especially fill factor of the organic solar cell devices were more improved which led to improvement of the overall power conversion efficiency (PCE).

References

[1] *Organic Photovoltaics: Concepts and Realization*, C. J. Brabec, V. Dyakonov, J. Parisi, and N. S. Sariciftci, Springer: Heidelberg, (2003).

[2] C. J. Brabec, N. S. Sariciftci, and J. C. Hummelen, *Adv. Funct. Mater. 11*, 15, (2001).

[3] S. E. Shaheen, C. J. Brabec, and N. S. Sariciftci, *Appl. Phys. Lett. 78*, 841, (2001).

[4] P. W. M. Blom, M. J. M. de Jong, and M. G. van Munster, *Phys. Rev. B 55*, R656, (1997).

[5] P. Peumans and S. R. Forrest, *Appl. Phys. Let. 79*, 126, (2001).

[6] G. Yu, J. Gao, J. C. Hummelen, F. Wudl, A. J. Heeger, *Science. 270*, 1789, (1995).

[7] N. S. Sariciftci, L. Smilowitz, A. J. Heeger, F. Wudl, *Science. 258*, 1474, (1992).

[8] P. Peumans, S. Uchida, and S. R. Forrest, *Nature. 425*, 158, (2003).

[9] W. L. Ma, C. Y. Yang, X. Gong, K. Lee, and A. J. Heeger, *Adv. Funct. Mater. 15*, 1617, (2005).

[10] B. Kraabel, J. C. Hummelen, D. Vacar, D. Moses, N. S. Sacriciftci, A. J. Heeger, and F. Wudl, *J. Chem. Phys. 104*, 4267, (1996).

[11] G. Li, C. W. Chu, V. Shrotriya, J. Huang, and Y. Yang, *Appl. Phys. Lett. 88*, 253503, (2006).

[12] M. M. Wienk, M. G. R. Turbiez, M. P. Struijk, M. Fonrodona, and R. A. J. Janssen, *Appl. Phys. Lett. 88*, 511, (2006).

[13] Y. Shao and Y. Yang, *Adv. Mater. (Weinheim, Ger.) 17*, 2841, (2005).

[14] M. Lenes and L. J. A. Koster, *Appl. Phys. Lett. 88*, 243502, (2006).
[15] L. S. Hung, C. W. Tang, and M. G. Mason, *Appl. Phys. Lett. 70*, 152, (1997).
[16] J. Yoon, J. J. Kim, T. W. Lee, and O. O. Park, *Appl. Phys. Lett. 76*, 2152, (2000).
[17] H. Hoppe, M. Niggemann, C. Winder, J. Kraut, E. Hiesgen, A. Hinsch, D. Meissner, N. S. Sariciftci, *Adv. Funct. Mater. 14*, 1005, (2004).
[18] D. Chirvase, J. Parisi, J. C. Hummelen, V. Dyakonove, *Nanotechnology. 15*, 1317, (2004).
[19] C. J. Brabec, S. E. Shaheen, C. Winder, and N. S. Sariciftci, *Appl. Phys. Lett. 80*, 1288, (2002).